ORIGINAL ARTICLE

A multi-criteria decision analysis for groundwater potential evaluation in parts of Ibadan, southwestern Nigeria

Olawale Olakunle Osinowo[1] · Kolawole Isaac Arowoogun[1]

Abstract

Multi-criteria decision analysis based on Saaty's analytical hierarchy processing technique has been used to establish groundwater potential distribution pattern across some highly populated parts of Ibadan metropolis in southwestern Nigeria. The technique weighted and ranked seven sets of thematic hydrological parameters derived from Landsat 8 OLI satellite imagery, 143 vertical electrical sounding (VES) geophysical data, and geological and topographical data. Filtered and enhanced Landsat 8 OLI satellite imagery, quality-checked and inverted VES data, and categorized geological and other ancillary data were analyzed and used to generate lineaments, subsurface geoelectric parameters and other terrain information employed to extract thematic hydrogeological parameters used to characterize the subsurface in terms of groundwater potential. Weighted, normalized and ranked derived thematic hydrogeological parameters (lineament density, drainage density, coefficient of anisotropy, aquifer thickness, overburden thickness, aquifer resistivity and lithology) were employed to generate groundwater resource potential map. The map delineates the study area into very low (6.5%), low (41.0%), medium (38.1%), high and very high (14.4%) groundwater resource potential zones. Regions underlain by quartzite/quartz schist rocks present medium-to-high groundwater resource potential, while regions underlain by migmatite and granite gneiss rocks mostly have very low–low groundwater resource potential. This study indicates that variation in groundwater resource potential across Ibadan situated within the basement complex terrain is mostly influenced by the heterogeneity of subsurface geology which varies rapidly in terms of rock distribution and associated hydrogeological indices.

Keywords Multi-criteria decision analysis (MCDA) · Analytical hierarchy process (AHP) · Vertical electrical sounding (VES) · Hydrogeological indices

Introduction

Water is an indispensable resource for human existence and is vital for social and economic growth. Increasing population, industrialization and changing consumption pattern have contributed to the global demand for water (WWAP 2015). The 2017 World Health Organization (WHO)/ United Nations and International Children Emergency Fund (UNICEF) Joint Monitoring Programme (JMP) report shows that about 2.1 billion people of the world inhabitants, most of which are in sub-Saharan Africa, require access to drinking water. This makes food security encompassing a high quest for potable water from a major part of the sustainable development goals (UN SDG 6 2018).

Surface water sources such as stream, river and lake, despite their abundances, can no longer meet up to the global demand as many of them dry up during the dry season, the condition which has been exacerbated by the climate change challenge. Ibadan is a densely inhabited city in sub-Saharan Africa, where rapid increase in urbanization demands better social amenities like potable water supply for industrial and domestic needs. The increasing population of students and staff of The Polytechnic Ibadan and the University of Ibadan campuses within the study area has imposed a lot of stress on the existing water supply scheme in these institutions. Hand-dug wells in the area which serve as alternatives are only productive during the wet season and at best low yielding during the dry season. It is therefore imperative to widen the exploration and development of groundwater within the study area for domestic and industrial use.

✉ Olawale Olakunle Osinowo
waleosinowo@gmail.com; waleosinowo@ui.edu.ng;
olawale.osinowo13@alumni.imperial.ac.uk

1 Department of Geology, University of Ibadan, Ibadan, Nigeria

Spatial problems like groundwater exploration is a multiple attribute decision-making challenge as it involves a group of factors that are appraised on the core of competitive and disproportionate criteria (Malczewski 1999). The integration of these various factors helps in developing a reliable and valid prediction map for future planning of groundwater exploitation within the area. This integration can be achieved through the use of multi-criteria decision analysis (MCDA). Multi-criteria decision analysis is a knowledge-driven, mathematical-based system that allows decision making between two or more contradictory alternatives. It also helps decision maker(s) to opt for the best option from a list of available substitutes and among competing criteria (Adiat 2013). Analytical hierarchy process (AHP) is the most commonly used MCDA method. AHP has recently found application in several fields of geology and more importantly in groundwater-related studies and has performed satisfactorily, especially in delineating groundwater potential zones (Adiat 2013; Fashae and Tijani 2014; Mogaji et al. 2014; Adiat et al. 2018).

Multi-criteria decision analysis was employed in this study to develop a groundwater potential assessment map of part of Ibadan metropolis. This part of Ibadan metropolis lies between latitudes 7° 25′ 00″ and 7° 28′ 00″ and longitudes 3° 51′ 00″ and 3° 55′ 00″ in southwestern Nigeria (Fig. 1). The groundwater potential assessment map was achieved through the integration of remotely sensed data, geoelectrical and geological parameters among others which were assumed to be controlling groundwater distribution in the area.

Geology of the study area

The study area is situated within the Precambrian basement complex rocks of southwestern Nigeria which lies within the Nigerian basement complex. The Nigerian basement complex itself belongs to the Pan-African mobile belt that lies east of the West African Craton (Russ 1957; Grant 1969, 1970; Oyawoye 1972; Burke et al. 1976; McMurry 1976; Odeyemi 1981; Toteu et al. 1991). The Nigerian basement complex was reported to be comprised of two major rock groups: the Metaigneous (i.e. quartzite, amphibolites and banded gneiss, mica schist, quartz schist and amphibolites schist) and Older Granite group (i.e. granite gneiss, migmatite, biotite granite, porphyritic granite and granodiorite) which were further subdivided into four major rock types: (a) Migmatite–Gneiss complexes, (b) Schist Belt, (c) Older Granites and (d) Younger Granite alkaline ring complexes

Fig. 1 Location and topographic map of the study area
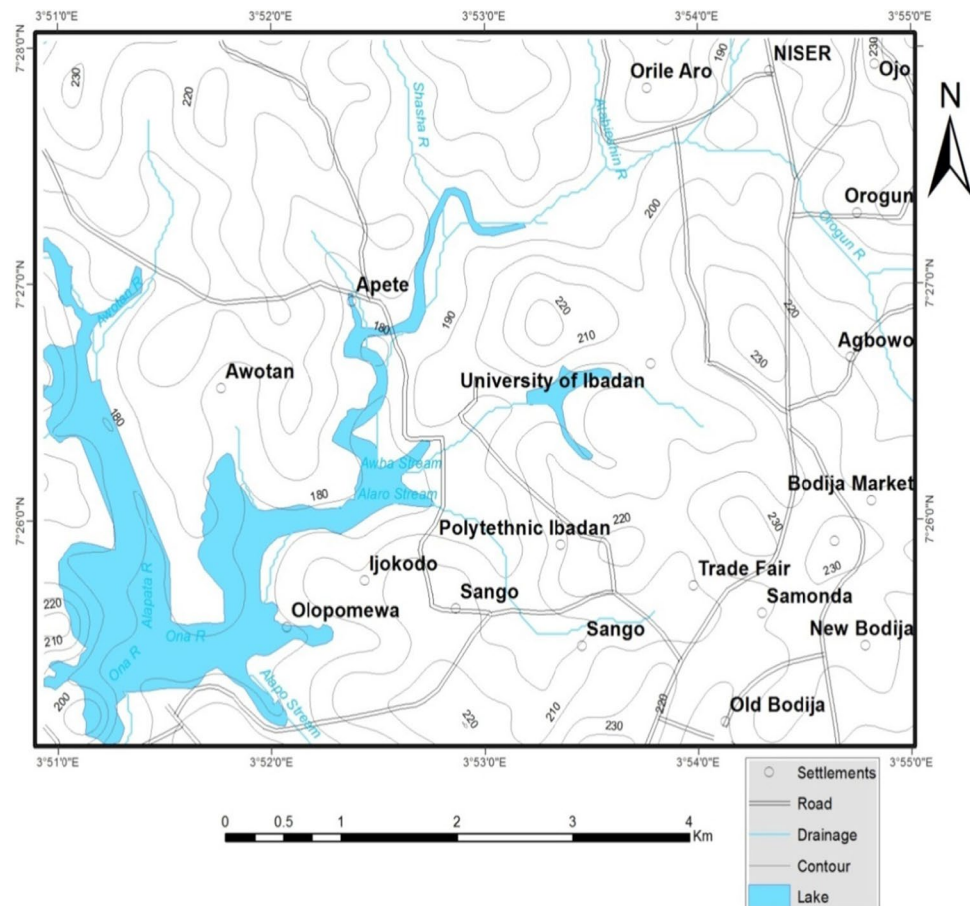
and volcanic rocks (Jones and Hockey 1964; Oyawoye 1972; Rahaman 1976; Ajibade 1980).

The basement complex of southwestern Nigeria consists of two distinct provinces, namely the eastern and the western provinces. The eastern province is characterized by Migmatite, Gneisses and large volumes of Pan-African Granites, intruded by the Mesozoic Younger Granites. The western province on the other hand comprised mostly low-grade Schist Belt, migmatite and gneisses or granites. The western basement complex rocks can be differentiated into the northwest and southwest zones. The southwest segment differs from the northwest in that the schist in the former is of lower grade and does not form well-defined belt like the northwest (Oyawoye 1972; Ajibade 1980).

The Ibadan metropolis occurs within the southwest zone of the basement complex of southwestern Nigeria. Major rock types in Ibadan are the undifferentiated meta-sediments which are quartzite of the meta-sediment series, migmatite–gneiss complex comprising banded gneiss, augen gneiss, granite gneiss and migmatites. However, the schist and the quartz schist are common and well exposed within the metropolis with several pegmatites, quartz veins, aplite and doleritic intrusions (Jones and Hockey 1964; Burke et al. 1976) (Fig. 2).

Materials and methods

In this study, different types of information were combined and analyzed using MCDA to characterize the study area into different groundwater potential zones. The different methods employed to generate the required information as well as how they were integrated and analyzed using the MCDA technique are presented in this section.

Ancillary data and satellite imagery

The ancillary data employed in this study include topographical and geological maps of the study area. The topographic map was extracted from the topographical map of Ibadan sheet 243. ArcGIS 10.3 was used to extract topographical features of the study area. The geological map was digitized using ArcGIS 10.3 to show the major rock types in the area.

Landsat Enhanced Thematic Mapper Plus 8 imagery covering the study area (Landsat 8 OLI) was acquired from Global Land Survey (GLS) facility of the University of Maryland, USA. The obtained imagery data were filtered using 3×3 prewitt edge detection tool which after linear stretching performs a 3×3 prewitt edge detection filtering on the raster image. This identifies areas of high slope in

Fig. 2 Geological map of the study area
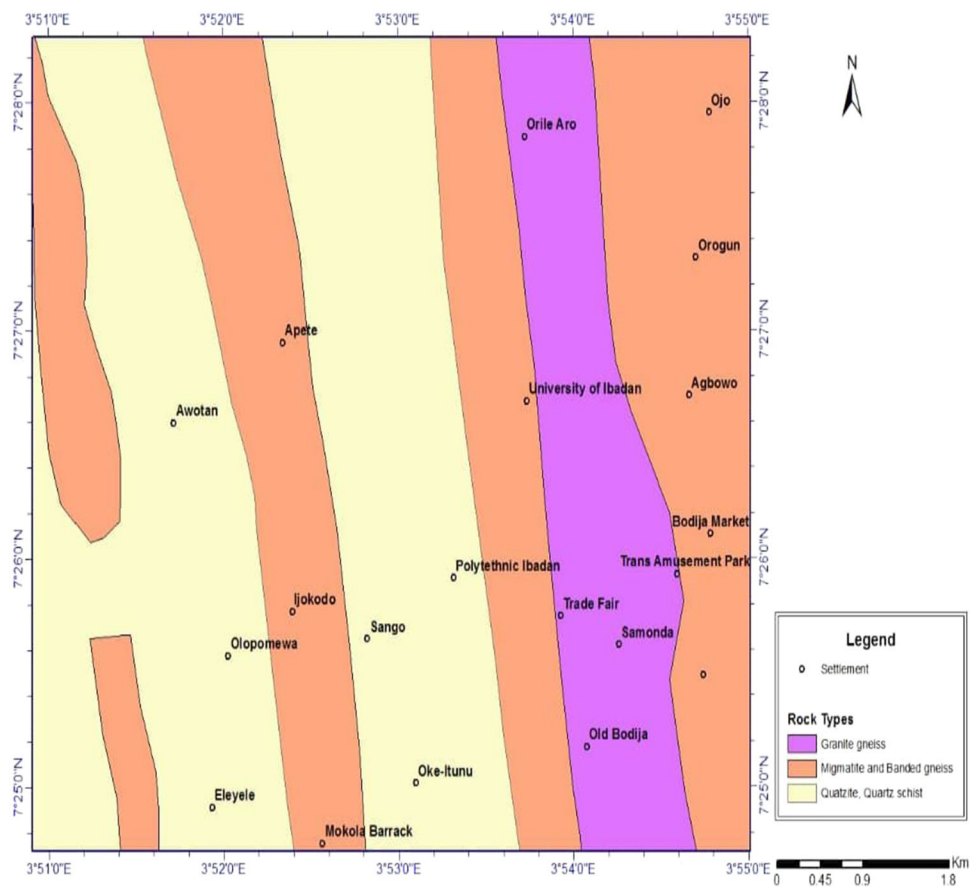
the input image through the calculation of slope in the *x* and *y* directions. Lineaments were subsequently extracted from the filtered image using the LINE module in PCI Geomatica tool. The extracted lineament was imported for various lineament corrections and thereafter employed to generate the lineament map of the study area. The lineament density of the study area was determined from the generated lineament map using ArcGIS 10.3 line density tool.

Geophysical data

Geoelectrical data acquisition involves occupying 143 vertical electrical sounding (VES) stations established along ten E-W profiles. An average of fifteen VES stations were occupied along each profile using Schlumberger array and with the aid of campus tiger resistivity meter (Fig. 3). This enables the generation of a 10×15 VES data grid across the study area. Georesistivity depth sounding for determination of the subsurface geoelectrical parameters at various occupied VES stations involves measurement of the generated potential difference which is the ground response to current flow within the subsurface across the electrode points. Current electrodes were spread from AB/2 of 1–240 m using the rule of thumb of 10% to 30% of surface electrode spread AB as the depth of investigation of VES (Loke 2000).

Multi-criteria decision analysis (MCDA) and analytical hierarchy process (AHP)

Multi-criteria decision analysis and analytical hierarchy process which is a formal, structured and transparent analytical decision-making technique that assists group or individual decision makers to explore their decision in a complex situation (Tecle and Duckstein 1994) was applied in this study. The techniques developed by Saaty (1980) are effective for solving problems associated with multifaceted decision making and apt at assisting in setting priorities in order to arrive at best unbiased decision. The decision making incorporates AHP as a functional method for evaluating the degree of consistency in decision maker's appraisals. The AHP examines a group of evaluation criteria and a group of alternative options from which the best decision is to be made. It thereafter assigns

Fig. 3 Map showing the VES points
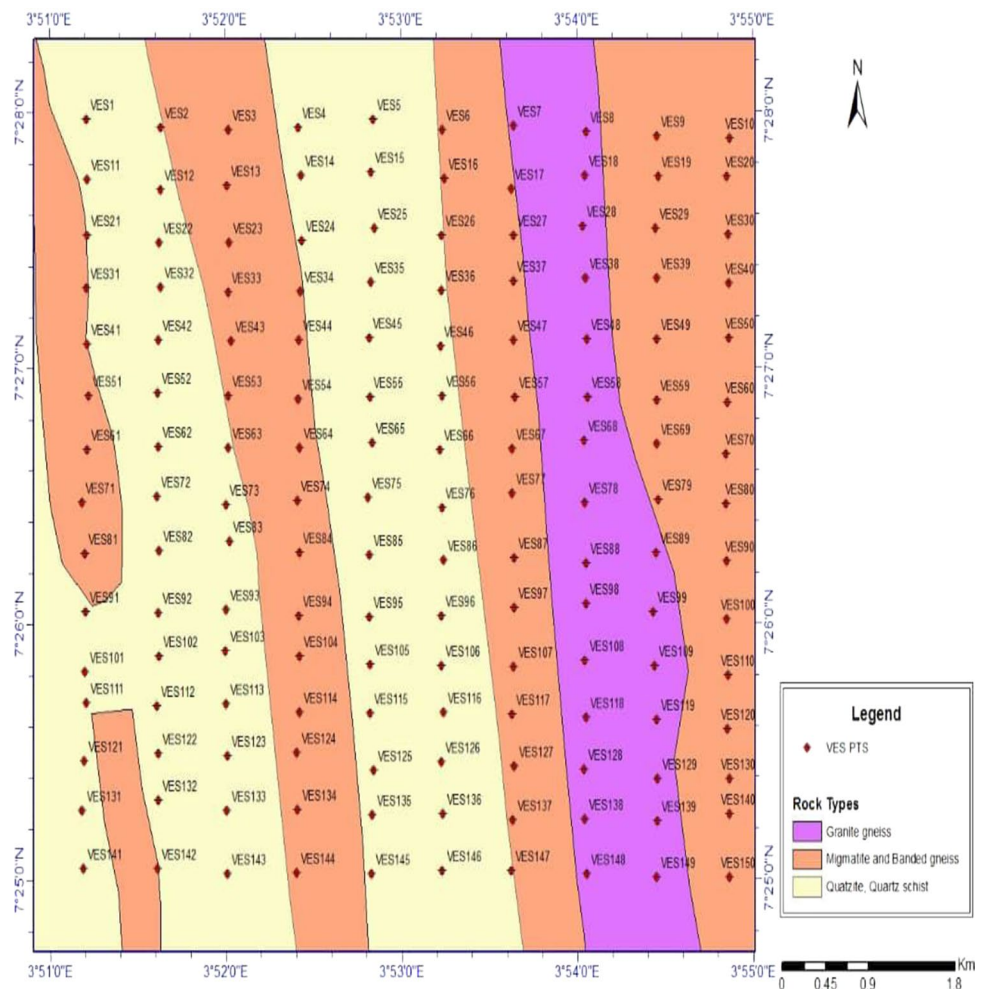
weights to the evaluating criteria using their relevance and afterward compared the resultant weights on the Saaty's nine-point comparison scale (1–3–5–7–9).

The Saaty's AHP produces a square matrix $\mathbf{A} = (a_{ij})$ for the criteria that are compared. The matrix $\mathbf{A}$ is reciprocal and consistent for each element a_{ij} of the matrix as expressed in Eq. 1.

$$aij = \frac{1}{aji} \tag{1}$$

For a reciprocal matrix, all the comparisons a_{ij} obey the equality, $ij = {P_i}/{P_j}$, and matrix P is the priority of the alternative i (2).

$$A = \begin{matrix} \frac{P1}{P1} & \cdots & \frac{P1}{Pj} & \cdots & \frac{P1}{Pn} \\ \cdots & 1 & \cdots & \cdots & \cdots \\ \frac{Pi}{P1} & & 1 & \cdots & \frac{Pi}{Pn} \\ \frac{Pn}{P1} & \cdots & \frac{Pn}{Pj} & \cdots 1 & \frac{Pn}{Pn} \end{matrix} \tag{2}$$

For this study, each thematic layer was reclassified using the reclassifying tool of the ArcGIS 10.3 software environment, to generate maps suitable for the AHP analysis. The weight of thematic layers is derived from the relative ratio scale derived from pairwise comparison reciprocal matrix of judgments and implemented in three consecutive steps.

First, all the elements of the column j of the matrix $\mathbf{A}$ are summed to give:

$$\frac{P1}{Pj} + \cdots + \frac{Pi}{Pj} + \cdots + \frac{Pn}{Pn} = \frac{\sum_{i=1}^{n} Pi}{Pj} \tag{3}$$

1. Then, the normalized value in column j is calculated by dividing the comparison $a_{ij} = P_i/P_j$ by Eq. (3)

$$\frac{\frac{Pi}{Pj}}{\frac{\sum_{i=1}^{n} Pi}{Pj}} = \frac{Pi}{Pj} \times \frac{Pj}{\sum_{i=1}^{n} Pi} = \frac{Pi}{\sum_{i=1}^{n} Pi} \tag{4}$$

Thereafter, the rate weight of row i is the average of the elements of the row i.

$$Wi = \left(\frac{Pi}{\sum_{i=1}^{n} Pi} + \cdots + \frac{Pi}{\sum_{i=1}^{n} Pi} \right) \times \frac{1}{n} \tag{5}$$

The consistency of the matrix was evaluated, as there may be prejudice in judgment for estimating weights, where n is the number of criteria to be evaluated.

$$\max = \sum_{i=1}^{n} \left(Wi \times \frac{Pi}{\sum_{i=1}^{n} Pi} \right) \tag{6}$$

The Consistency Index (CI) was evaluated from the principal eigenvector (λ), and n is the number of criteria to be adjudged. CI is expressed mathematically in Eq. (7).

$$CI = \frac{\lambda \max - n}{n - 1} \tag{7}$$

The Consistency Ratio (CR) measures the prejudice of the pairwise comparison matrix of evaluating criteria as emphasize by Saaty (1980).

$$CR = \frac{CI}{RI} \tag{8}$$

CI was evaluated based on the principal eigenvalue (λ_{max}) (Saaty 1990; Malczewski 1999), where Random Index (RI) varies with the number of criteria evaluated (Saaty 1977). Here, CR < 10%, then the matrix is said to be within acceptable limits and as such can be used in decision and judgment making. If otherwise, the comparison matrix would be re-evaluated.

Finally, groundwater potential map of the study area was generated using the weighted overlay method in ArcGIS 10.3. The layers used in this study are lineament density, drainage density, coefficient of anisotropy, aquifer thickness, overburden thickness, aquifer resistivity and lithology. The maps generated from all the layers were used for weighted analysis; the individual raster layer was reclassified. Weight and rank were assigned based on Saaty's Analytical Hierarchical Process. The weights and ranks were determined by the relative contribution of each thematic layer to the movement and storage of groundwater in the study area.
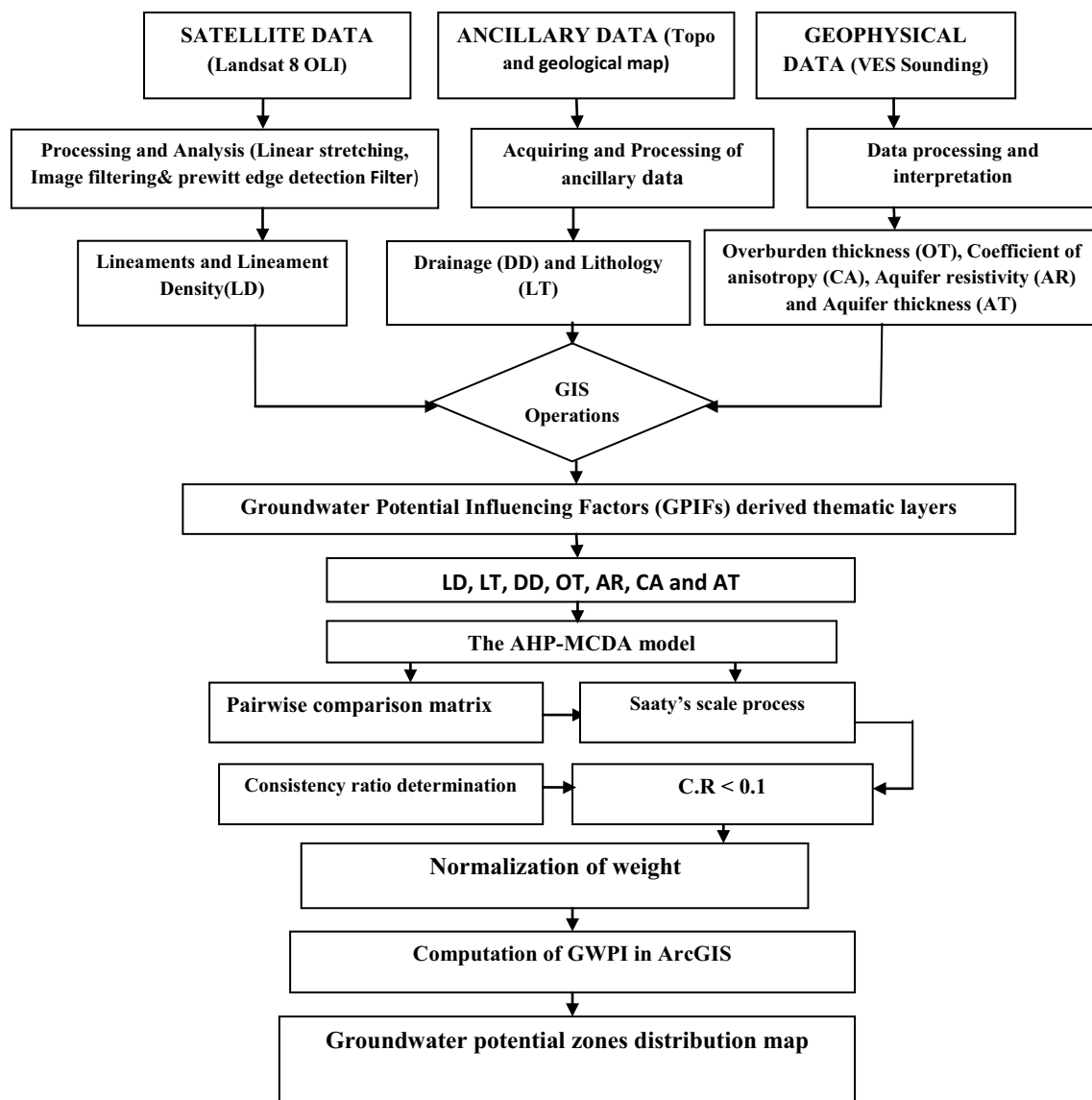
A simplified flow diagram illustrating the different steps employed to integrate data, process, evaluate and analyze the combined information for groundwater potential evaluation of the part of Ibadan metropolis is presented in Fig. 4.

Results and discussion

The various factors influencing the groundwater potential of the study area and other relevant subsurface information obtained in respect of the groundwater resource potential of some parts of Ibadan metropolis in southwestern Nigeria are presented and discussed in this section.

Interpretation of ancillary data and satellite imagery

Lineaments, which are surficial representation of linear features such as fractures and dykes, are easily identified on satellite imagery and play a vital role in groundwater storage, especially in a crystalline basement environment. The extracted lineaments from the Landsat OLI satellite imagery

```
┌──────────────────────┐  ┌──────────────────────┐  ┌──────────────────────┐
│   SATELLITE DATA     │  │ ANCILLARY DATA (Topo │  │   GEOPHYSICAL        │
│  (Landsat 8 OLI)     │  │  and geological map) │  │ DATA (VES Sounding)  │
└──────────────────────┘  └──────────────────────┘  └──────────────────────┘
           │                         │                         │
           ▼                         ▼                         ▼
┌──────────────────────┐  ┌──────────────────────┐  ┌──────────────────────┐
│ Processing and       │  │ Acquiring and        │  │ Data processing and  │
│ Analysis (Linear     │  │ Processing of        │  │ interpretation       │
│ stretching, Image    │  │ ancillary data       │  │                      │
│ filtering& prewitt   │  │                      │  │                      │
│ edge detection       │  │                      │  │                      │
│ Filter)              │  │                      │  │                      │
└──────────────────────┘  └──────────────────────┘  └──────────────────────┘
           │                         │                         │
           ▼                         ▼                         ▼
┌──────────────────────┐  ┌──────────────────────┐  ┌──────────────────────┐
│ Lineaments and       │  │ Drainage (DD) and    │  │ Overburden thickness │
│ Lineament            │  │ Lithology            │  │ (OT), Coefficient of │
│ Density(LD)          │  │ (LT)                 │  │ anisotropy (CA),     │
│                      │  │                      │  │ Aquifer resistivity  │
│                      │  │                      │  │ (AR) and Aquifer     │
│                      │  │                      │  │ thickness (AT)       │
└──────────────────────┘  └──────────────────────┘  └──────────────────────┘
```

Groundwater Potential Influencing Factors (GPIFs) derived thematic layers

LD, LT, DD, OT, AR, CA and AT

The AHP-MCDA model

Pairwise comparison matrix → Saaty's scale process

Consistency ratio determination → C.R < 0.1

Normalization of weight

Computation of GWPI in ArcGIS

Groundwater potential zones distribution map

Fig. 4 Simplified flow diagram showing various steps adopted to generate groundwater potential distribution map of the study area

are presented in Fig. 5. It shows linear features which present fairly radial pattern some of which are relatively long extending up to 4 km in length. Figure 6 shows the lineament density map generated from the lineament map which was itself derived from the satellite imagery of the area. The lineament density map which presents a measure of the constellation of lineaments in an area indirectly reveals the presence of features capable of storing and transmitting groundwater. Relatively high lineament density characterized the northeastern (NE) and southwestern (SW) parts of the study area with the lineaments generally trending NNE-SSW in conformity to the trend of Pan-African orogeny. The derived lineaments and the lineament density maps indicate medium groundwater potential with slightly higher potential in the NE and SW parts of the study area which are underlain by

quartzites/quartz schist, as different from the low-to-medium linear density in areas underlain by migmatite and banded gneiss.

Rock composition and distribution which define formation porosity and permeability largely influence rock's aquifer properties and thus control water infiltration, storativity and by extension groundwater resource potential (Chowdhury et al. 2003). Generally, basement complex rocks which have very low primary porosity and permeability as a result of the interlocking nature of the individual crystals of crystalline rocks present relatively limited groundwater potential, especially when compared to clastic sedimentary rocks. The study area is underlain by migmatite and banded gneiss which runs in a north–south direction across the study terrain, occupying 49.2% of the

Fig. 5 Lineament map of the study area
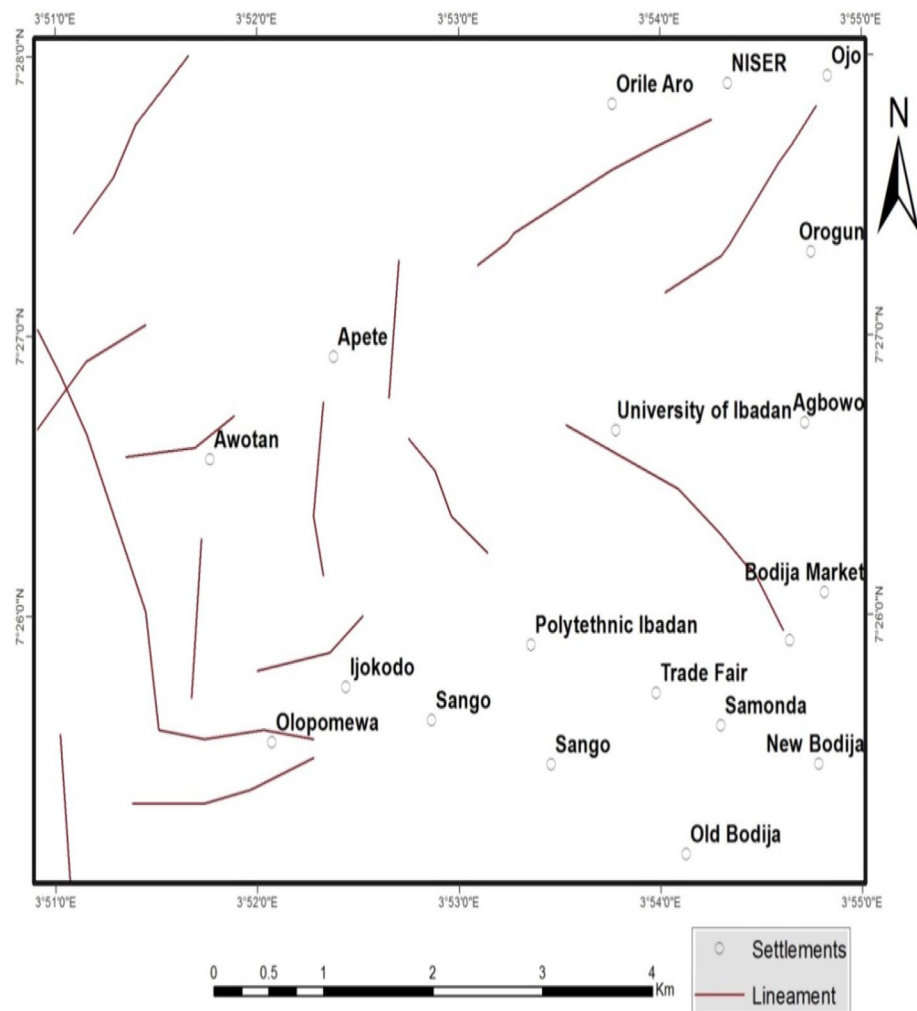
study area. Granite gneiss on the other hand covers 15.6% of the area, while quartzite/quartz schist spread across 35.2% of the entire study area (Fig. 3). Judging from the resistance of the different rock types across the study area to weathering and consequently, their contribution to groundwater potential, quartzite/quartz schist has the lowest resistance to weathering and hence has the highest potential for groundwater while migmatite/banded gneiss exhibit the highest resistance to fracturing/weathering hence has the lower groundwater resource potential.

The drainage density map (Fig. 7) generated from the drainage distribution of the area (Fig. 1) was also used as the groundwater potential indicator in this study. Dendritic drainage density pattern which reflects relatively high drainage indicates relatively high run-off that suggests reduced infiltration and aquifer. Generally, the study area is not well drained and is expected to have medium-to-high groundwater potential except in the southwestern and northeastern part of the study area.

Geophysical data interpretations

The results generated from the interpretation of the georesistivity survey data are presented as sounding curves. Ten curve types were delineated, namely A, K, Q, H, KH, HA, QH, AK, HK and HKH. The most common curve types identified are the H, KH and HA curves with percentage abundance of 38.4%, 25.2% and 18.9%, respectively (Fig. 8). The representative curves obtained in the study are shown in Fig. 9a–h.

Coefficient of anisotropy

The weighted coefficient of anisotropy map of the study area (Fig. 10), generated from the Dar Zarrouk parameters (transverse resistance and longitudinal conductance), which is a veritable factor for assessing groundwater potential, was used to evaluate groundwater distribution pattern around basement complex terrain of the study area. Generally,

Fig. 6 Lineament density map of the study area
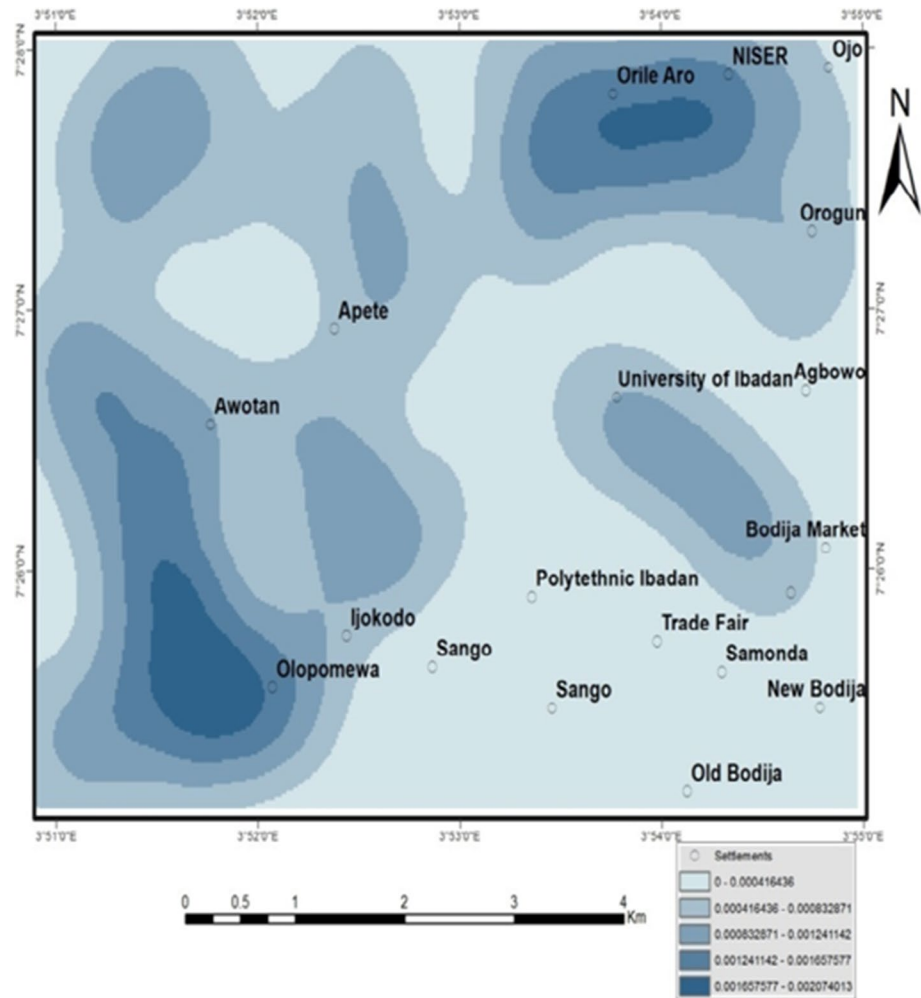
low-to-medium coefficient of anisotropy values which range from 1.00 to 2.93 was obtained from the anisotropy analysis of the study area. Low coefficient of anisotropy value implies low degree of fracturing and thus suggests low groundwater storage potential (Ritzi and Andolsek 1992; Forson and Whiteman 2014).

A considerable part of the study area presents low anisotropic value (1.00–1.25) with some isolated regions around Ijokodo, Sango, Orogun, Bodija, The Polytechnic Ibadan and University of Ibadan have relatively higher anisotropic coefficient (1.71–2.93). Zones of relatively high coefficient of anisotropy mostly correspond to regions of high lineament/fracture density. The anisotropic coefficient is an indirect measure of the degree of fracturing, thus implying the degree of fracturing is an important hydrological index favorable for groundwater storage (Knochenmus and Robinson 1996).

Aquifer thickness

Aquifer thickness, an important factor in aquifer characterization, was determined from the geophysical parameters, and it ranges in value from 1.02 to 45.5 m with average aquifer thickness of 13.60 m around the study area. The thickest and thinnest aquifers were recorded on quartzite/quartz schists and granite gneiss rocks, respectively. Here, areas underlain by quartzite/quartz schist generally present higher overburden and considerable aquifer thickness, while regions underlain by migmatite and granite gneiss show relatively thin overburden and consequently thin aquifer thickness. The average aquifer thickness on migmatite, granite gneiss and quartzite/quartz schist is 10.78, 10.79, and 17.6 m, respectively. Figure 11 presents the aquifer thickness distribution across the study area, indicating relatively thick aquifer in the central and southeastern part of the study area.

**Fig. 7** Drainage density map of the study area
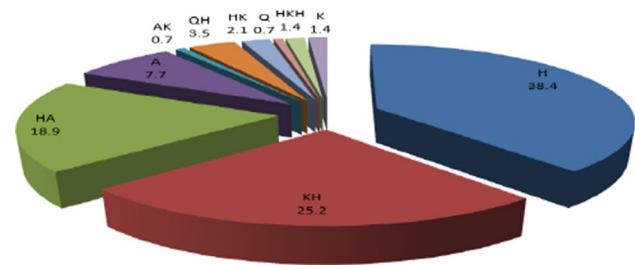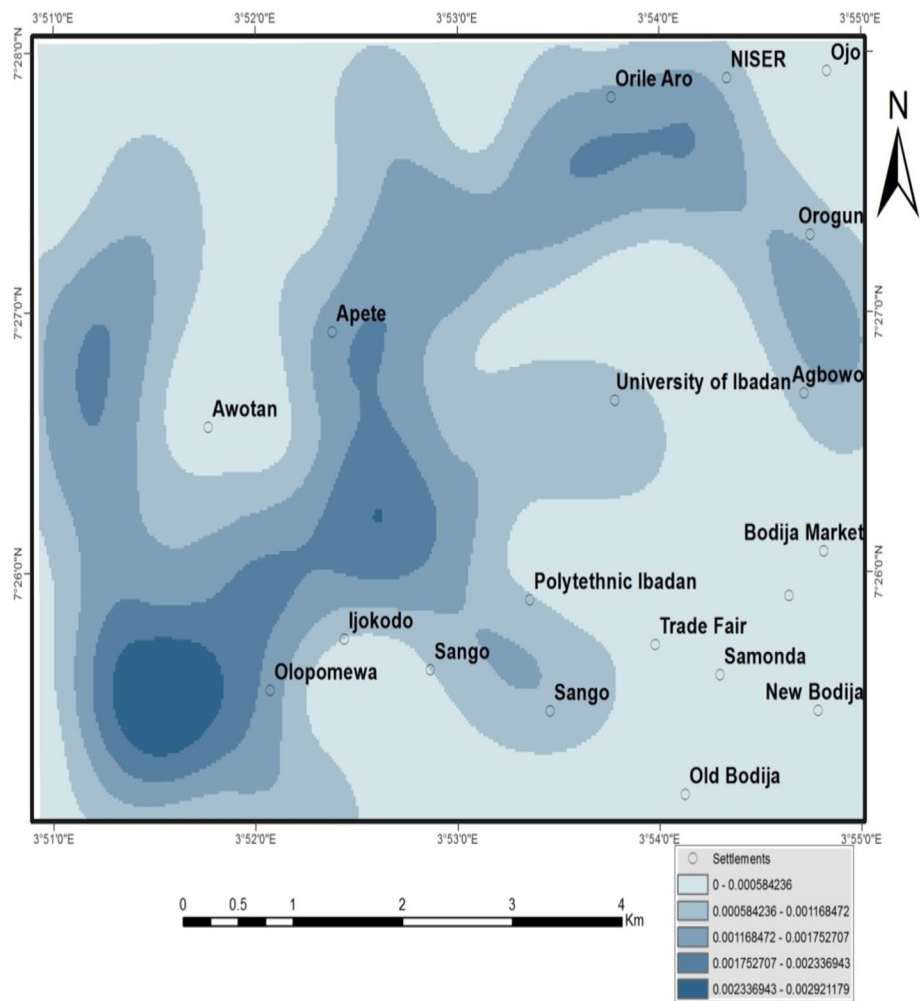
Fig. 8 Pie chart showing the distribution of curve types obtained from VES in the study area

Overburden thickness

Overburden thickness, the sum total of the materials overlying the fresh basement rocks, has been reported by several researchers to mostly influence groundwater storage capacity in the basement complex terrain. Areas of thick overburden are often region of comparative groundwater potential than region of less overburden cover, especially where the terrain is less fractured and the overburden material is less clayey

(Olorunfemi 1990; Olorunfemi et al. 1991; Omosuyi et al. 2003; Abdullahi et al. 2016). The overburden thickness map of the area generated from the overburden thickness values obtained from the various VES results across the study area is presented in Fig. 12. It indicates that overburden thickness over the basement complex rocks of southwestern Nigeria varies between 1.5 and 52 m across the study area with an average overburden thickness value of 17.60 m. The obtained overburden thickness distribution values agree with the earlier published values by Oyedele et al. (2013) and Abdullahi et al. (2016) for the basement complex in southwestern Nigeria. The generated overburden thickness map (Fig. 12) generally indicates thick overburden cover above the basement rocks in the southwest and central part of the study area. Regions underlain by quartzite and quartz schist are mostly characterized by relatively thick overburden cover, while relatively thin overburden cover occurs over migmatite–gneiss and banded gneiss terrain. This is likely associated with the fact that migmatite–gneiss exhibits higher resistance to weathering compared to the other rock types in the area.

Fig. 9 Representative **a** A, **b** Q, **c** K, **d** KH, **e** H, **f** HA, **g** HKH and **h** HK VES curves
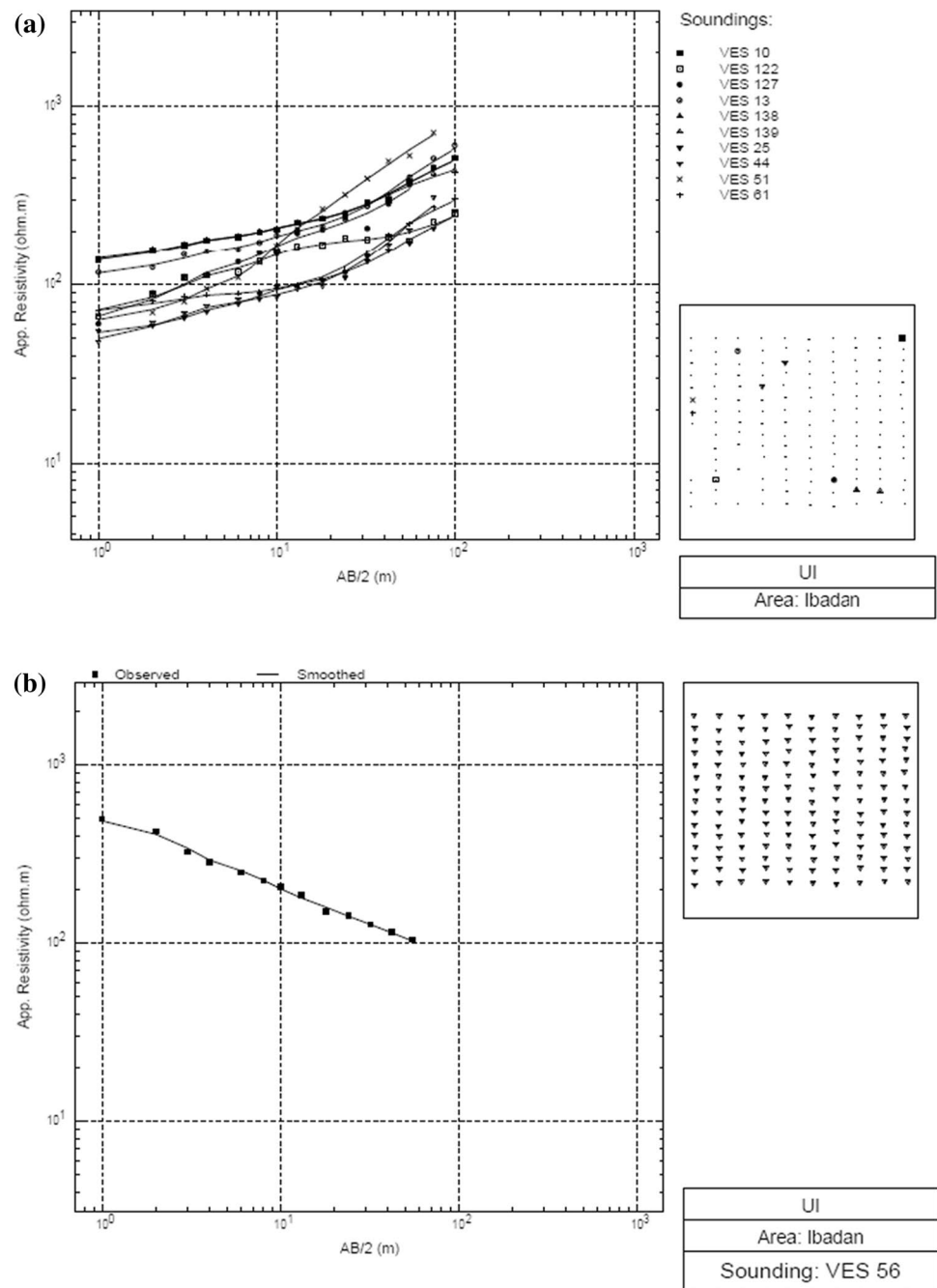

Aquifer resistivity

The aquifer resistivity, a parameter that measures the degree of rock resistance (resistivity/conductivity) to the flow of electric current within a geological formation, indirectly measures aquifer water saturation and thus useful for providing relevant information about groundwater potential of a geological terrain. Low aquifer resistivity inversely correlates with relatively high groundwater occurrence, with the exception of some low permeability rocks, such as clay, which may present low resistivity but poor groundwater quality (Akinlalu et al. 2017).

The aquifer resistivity map (Fig. 13) presents the aquifer resistivity distribution of the combined aquifer units (weathered and fractured) identified from the electrical resistivity survey of the area. The combined aquifer ranges in resistivity value from 15 to 1998 Ωm with a mean value of 123.16 Ωm across the study area. Low aquifer resistivity distribution generally characterizes the study area with the lowest values obtained in quartzite/quartz schist rocks which gives

Fig. 9 (continued)

(c)

(d)
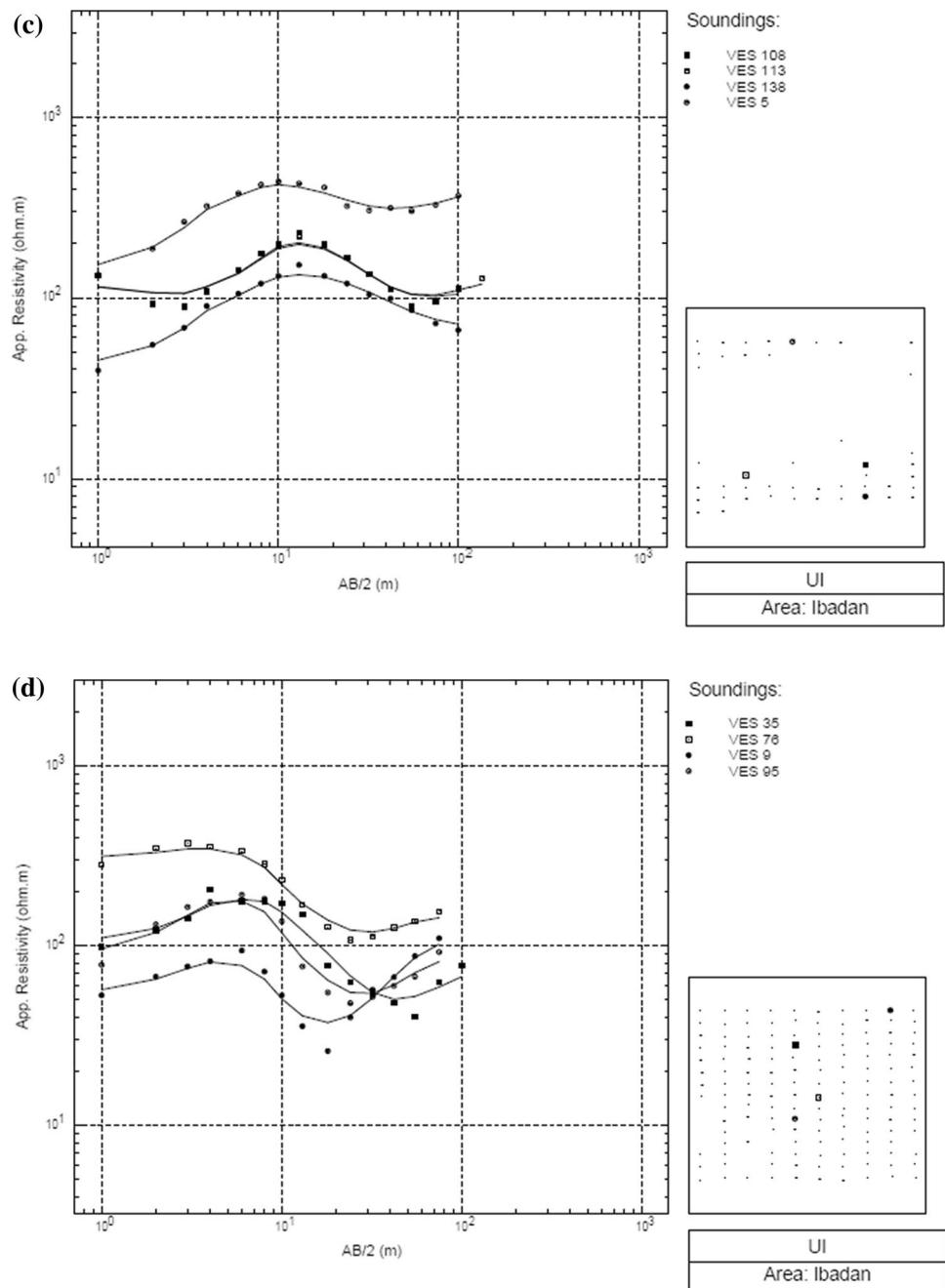
characteristic H-VES curve types, representative of intermediate to low resistivity due to relatively high saturation.

Multi-criteria decision analysis and analytical hierarchy process results

Pairwise comparison matrix aided weights factor assignment using Saaty's nine-point rating scale (Table 1) that compares parameters based on importance to groundwater occurrence.

In MCDA technique, the weights sum to 1 as proposed by Saaty (1980) as shown in Table 2. The normalized weights of the factors using the principal eigenvectors of the maximum eigenvalue of the pairwise comparison matrix assigned to the selected GPIFs for this study are presented in Table 3. Equation 9 generated the Groundwater Potential Index (GWPI) from the normalized weights.

$$GWPI = \sum WiRi \tag{9}$$

Fig. 9 (continued)
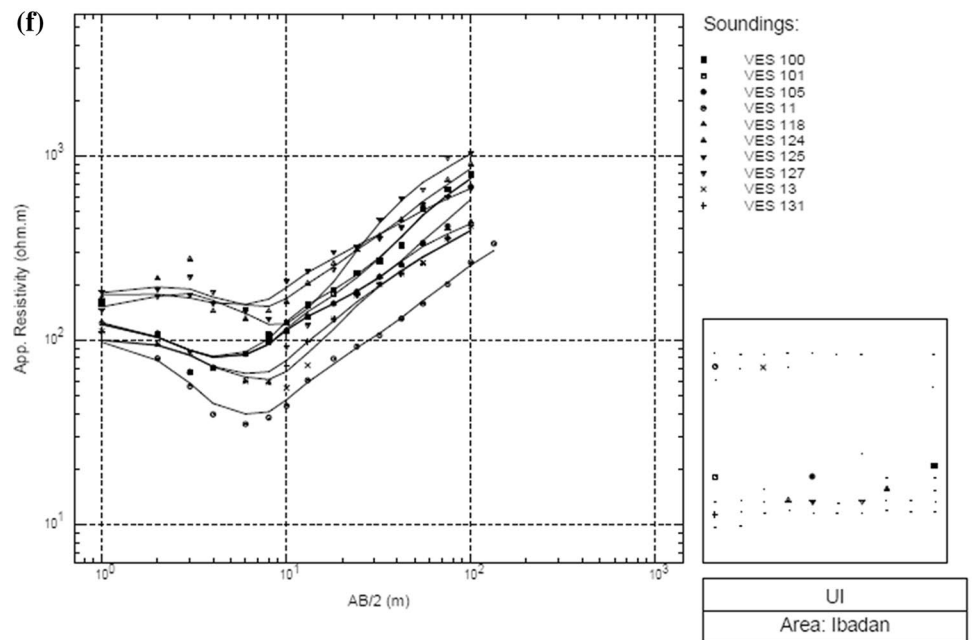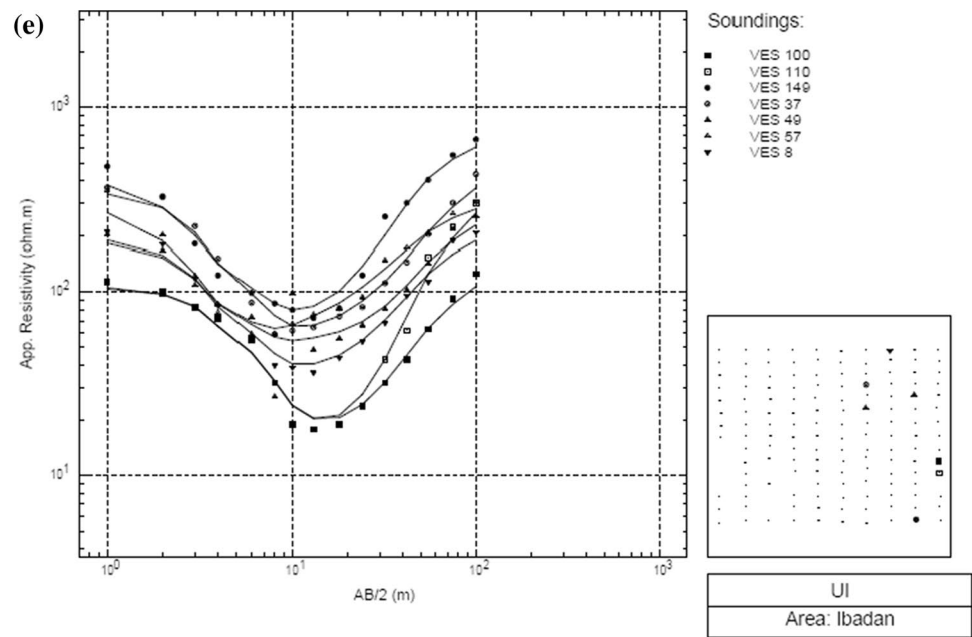
$$GWPI = 0.0229DdR + 0.1558LtR + 0.0583LdR + 0.0954CaR + 0.0374AtR + 0.2424ArR + 0.3878OtR \qquad (10)$$

where 'W' is the assigned weight and 'R' implies rating of each criteria. CaR = coefficient of anisotropy rating; LtR = lithology rating; LdR = lineament density rating; ArR = aquifer resistivity rating; AtR = aquifer thickness rating; OtR = overburden thickness rating; and DdR = drainage density rating. The AHP result has a consistency ratio of 8.03%.

Groundwater potential distribution map

Groundwater potential map of the study area generated through analytical hierarchy processing which involves ranking, assigning weight to all the various results such as drainage and lineament density, coefficient of anisotropy,

Fig. 9 (continued)

(g)

(h)
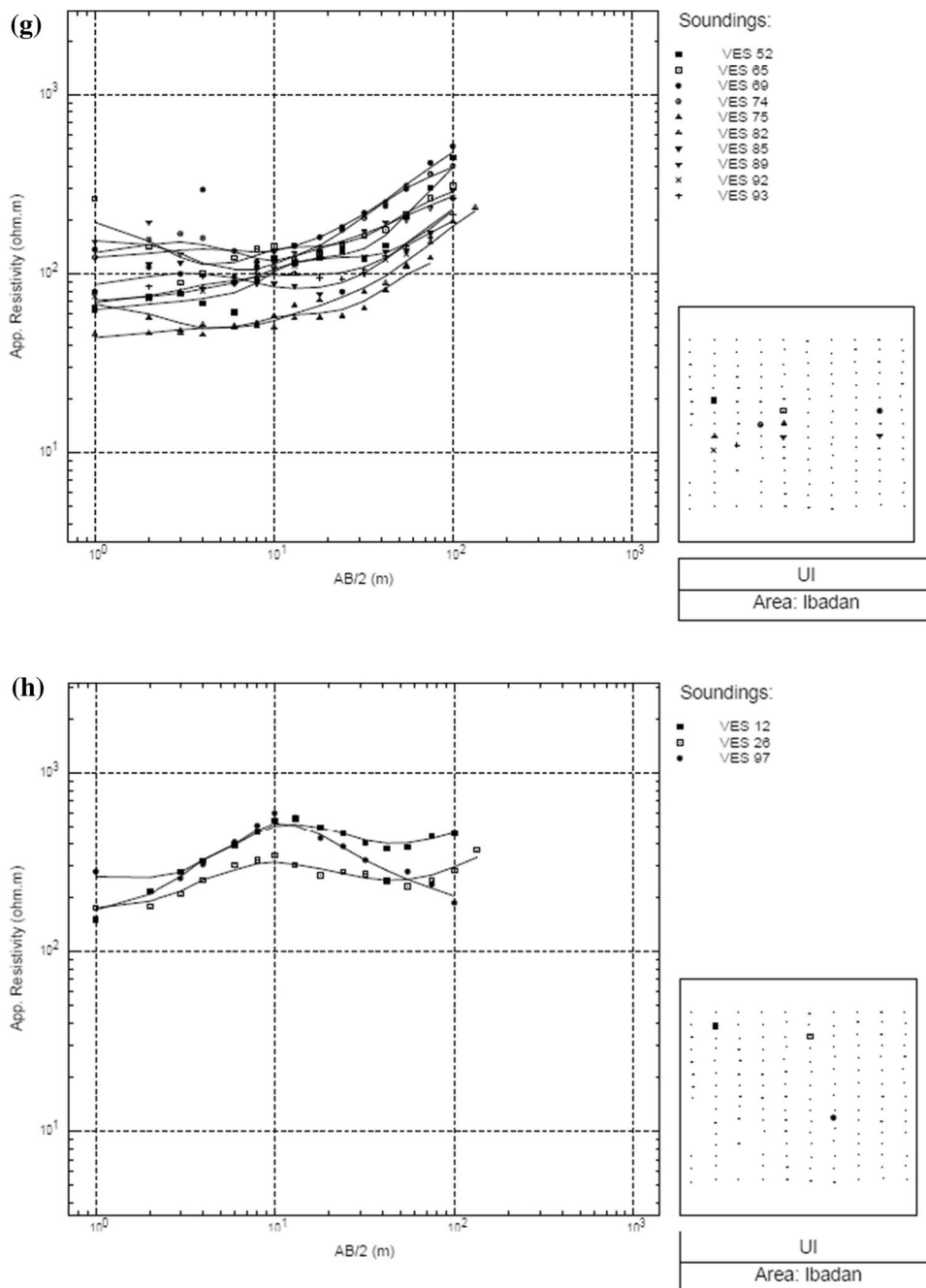
overburden thickness distribution, aquifer thickness and aquifer resistivity, derived directly or indirectly from remote sensing, geophysical survey, geological and ancillary data, for the purpose of generating different thematic layers of the map is presented in this section.
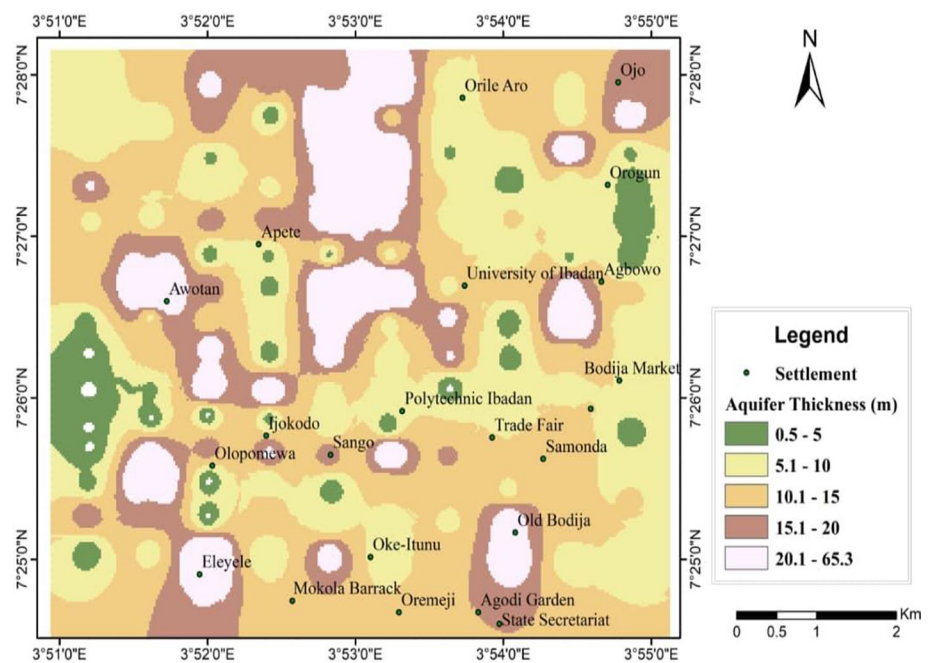
The generated groundwater potential map of the area produced by overlaying the resultant Groundwater Potential Index (GWPI) obtained from Eq. 9 using ArcGIS 10.3 software is presented in Fig. 14. The potential map classified the area into very low, low, medium and very high groundwater potential zones. The map (Fig. 14) indicates

that 6.47% of the total study area has very low groundwater potential, 41.01% has low potential, 38.13% has the medium potential, and 14.39% are categorized as having very high groundwater potential. Generally, the study area can be described as having low-to-moderate groundwater potential. The regions classified as having very low-to-low GWPI are found to be predominantly underlain by migmatite/banded gneiss. The medium groundwater potential zones are mainly underlain by granite gneiss, while the moderate-to-very high groundwater zones occur within quartzites and quartz schist terrain (Table 4).

Fig. 10 Coefficient of anisotropy map of the study area
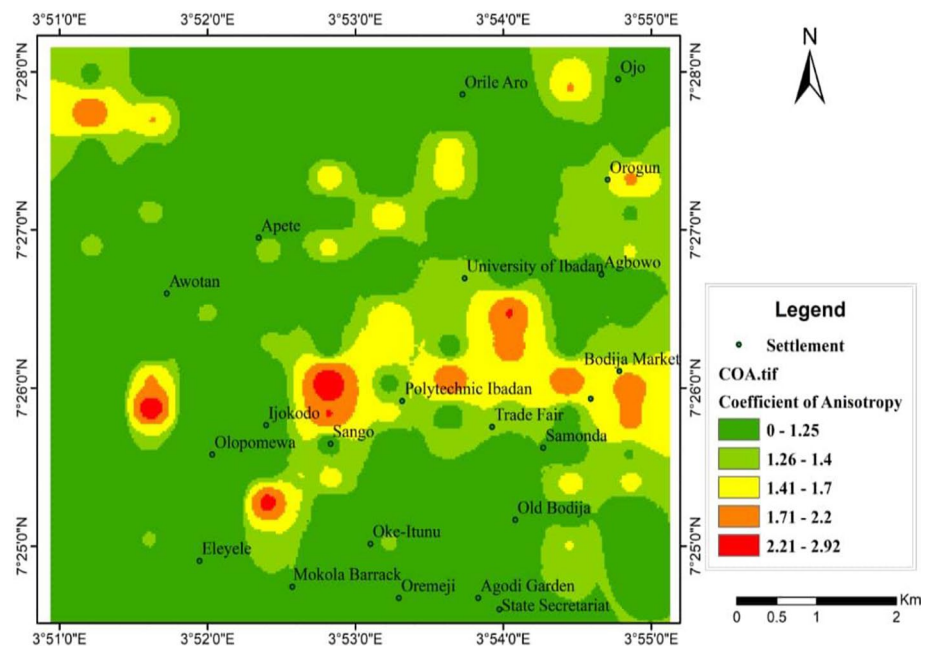
Fig. 11 Aquifer thickness map of the study area

Groundwater potential map validation with borehole/well data

The validation of the result with existing boreholes and wells information from the study area establishes the reliability of the groundwater potential model in the form of a groundwater potential map across the studied part of the Ibadan metropolis in southwestern Nigeria. The plot of the eight collected hand-dug water wells and eleven borehole points within the study area (provided by the Oyo State

Water and Sanitation Agency (WATSAN)) is presented in Fig. 15. Measurements such as static water level and yield from wells and boreholes used generated a table (Table 5) which compares the yield of the wells and borehole with the MCDA generated classification for groundwater potential of the study area. The table indicates that the yield of two of the hand-dug wells and three of the boreholes sampled which represents 26.32% disagree with the generated groundwater potential model, while the remaining 73.68% presented water yield that conforms with the projected groundwater
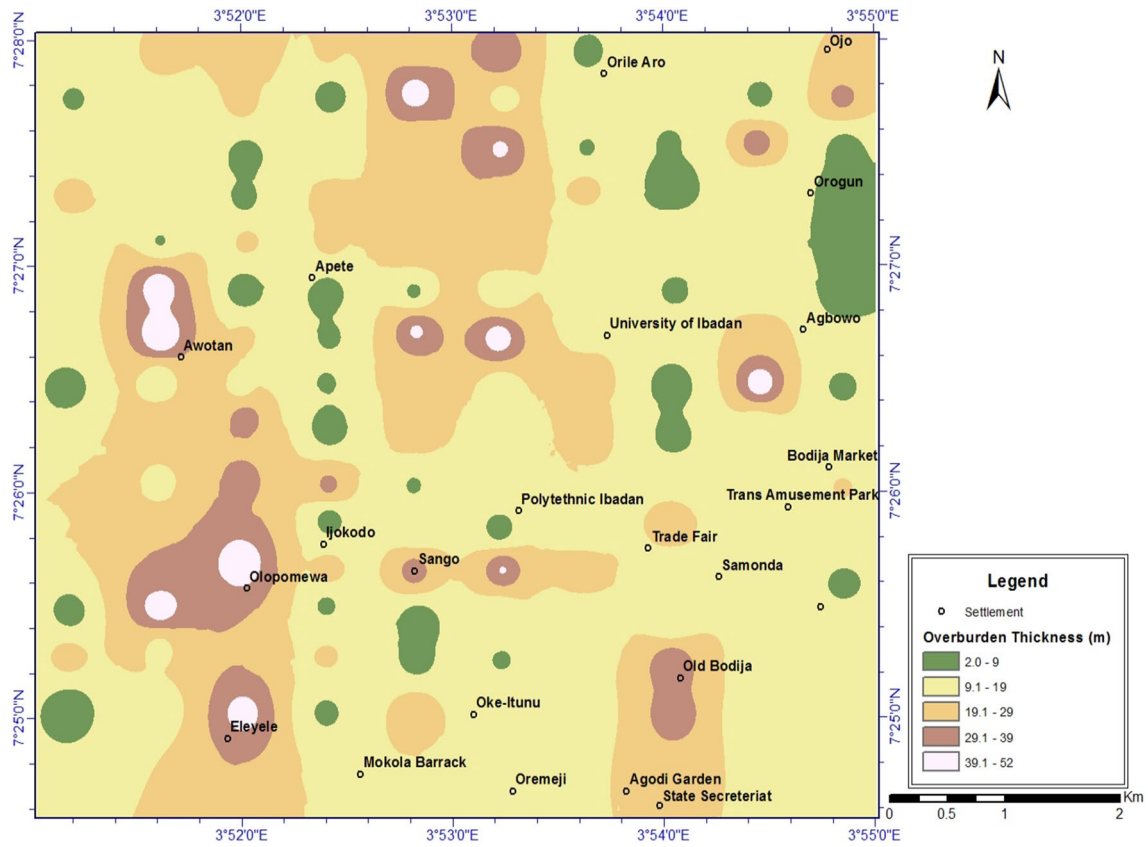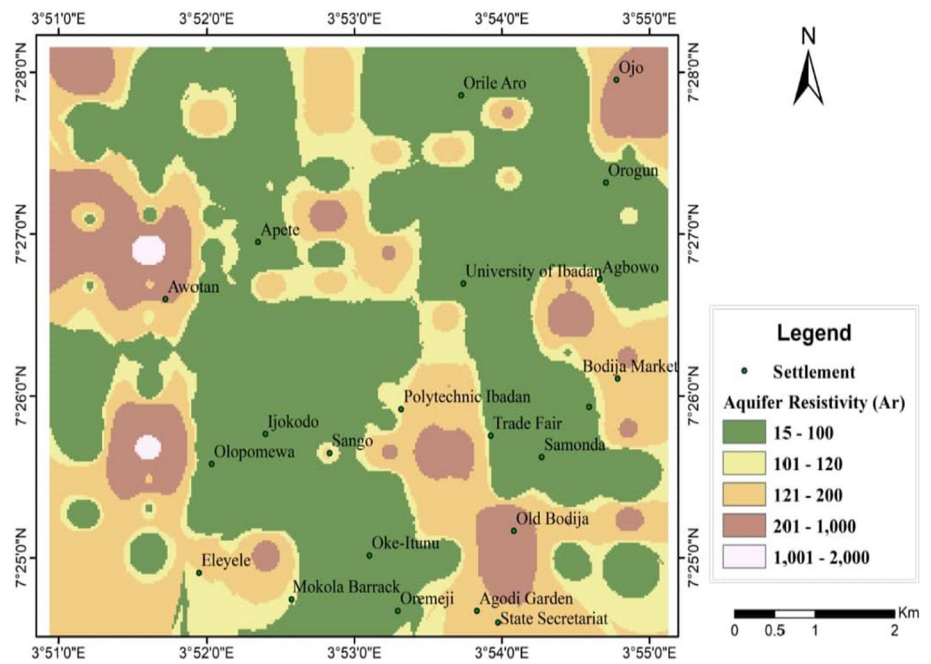
Fig. 12 Overburden thickness map of the study area

Fig. 13 Aquifer resistivity map of the study area

Table 1 Saaty's pairwise comparison nine-point rating scale

| Less important				Equally important	More important			
1/9	1/7	1/5	1/3	1	3	5	7	9
Extremely	Very strongly	Strongly	Moderately		Moderately	Strongly	Very strongly	Extremely

Table 2 Pairwise comparison matrix for the selected GPIFs

	CA	LT	LD	AR	AT	OT	DD
CA	1	0.333	3	0.333	3	0.2	5
LT	3	1	3	0.333	5	0.333	7
LD	0.333	0.333	1	0.2	3	0.1429	3
AR	3	3	5	1	7	0.333	9
AT	0.333	0.2	0.333	0.1429	1	0.111	3
OT	5	3	7	3	9	1	9
DD	0.2	0.1429	0.333	0.111	0.333	0.111	1
SUM	12.866	8.0089	19.666	5.1199	28.333	2.2309	37

Table 3 Relative weight for the GPIFs

	CA	LT	LD	AR	AT	OT	DD	$W = \frac{1}{n} \sum Wi$
CA	0.077724	0.041579	0.152548	0.06504	0.105884	0.08965	0.135135	0.095366
LT	0.233173	0.124861	0.152548	0.06504	0.176473	0.149267	0.189189	0.155793
LD	0.025882	0.041579	0.050849	0.039063	0.105884	0.064055	0.081081	0.058342
AR	0.233173	0.374583	0.254246	0.195316	0.247062	0.149267	0.243243	0.242413
AT	0.025882	0.024972	0.016933	0.027911	0.035295	0.049756	0.081081	0.037404
OT	0.388621	0.374583	0.355944	0.585949	0.317651	0.44825	0.243243	0.387749
DD	0.015545	0.017843	0.016933	0.02168	0.011753	0.049756	0.027027	0.022934
	1	1	1	1	1	1	1	1

The weight and ratings of the seven indices used in the study are summarized in Table 4

Fig. 14 Groundwater potential map of the study area
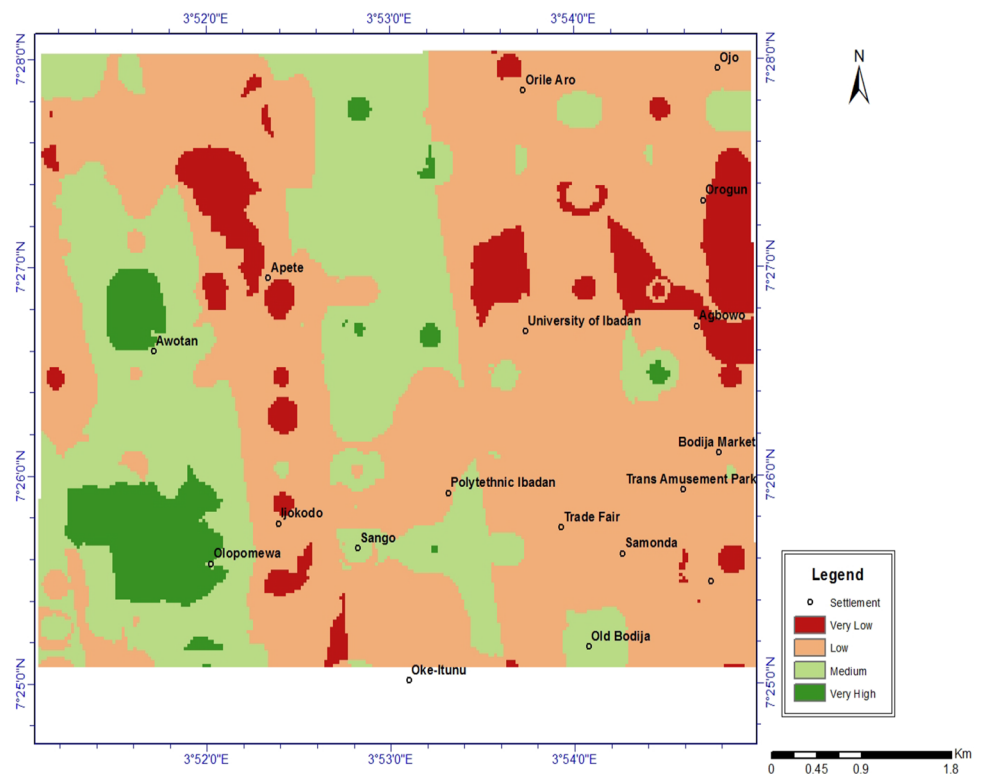
Table 4 Assigned and normalized weight of the GPIFs

| GPIFs	Classes	Potentiality	Rating	Normalized weight
Drainage density (Dd)	0.000000000–0.000584236	Very high	5	0.0229 (2.29%)
	0.000584236–0.001168472	High	4	
	0.001168472–0.001752707	Medium	3	
	0.001752707–0.002336943	Low	2	
	0.002336943–0.002921179	Very low	1	
Lineament density (Ld)	0.0000000000–0.000416436	Very low	1	0.0583 (5.83%)
	0.000416436–0.00832871	Low	2	
	0.00832871–0.001241142	Medium	3	
	0.001241142–0.001657577	High	4	
	0.001657577–0.002074013	Very high	5	
Aquifer resistivity (Ar)	15–100	Very low	1	0.2424 (24.24%)
	101–120	Low	2	
	121–300	Medium	3	
	301–1000	High	4	
	1001–2000	Very high	5	
Aquifer thickness (At)	1.02–5	Very low	1	0.0374 (3.74%)
	5.01–10	Low	2	
	10.01–14	Medium	3	
	15–20	High	4	
	20–70.61	Very high	5	
Coefficient of anisotropy (Ca)	1–1.25	Very low	1	0.0954 (9.54%)
	1.26–1.40	Low	2	
	1.41–1.70	Medium	3	
	1.26–1.40	High	4	
	2.21–2.93	Very high	5	
Overburden thickness (Ot)	2.09–9	Very low	1	0.3878 (38.78%)
	9.01–19	Low	2	
	19.01–29	Medium	3	
	29.01–39	High	4	
	39.01–72	Very high	5	
Lithology (Lt)	Quartzite/quartz Schist	Very high	5	0.1558 (15.58%)
	Granite gneiss Migmatite/	Medium	3	
	Banded gneiss	Very low	1	

potential of the area where the wells and boreholes were sampled.

Conclusions

The application of multi-criteria decision analysis to generate groundwater potential map of part of Ibadan metropolis in southwest Nigeria, through the combination of several thematic layers of information derived from analytical hierarchy processing, was demonstrated in this study. The analysis involves ranking and weighting of seven hydrological parameters, including geological parameters (lineament density, lithology and drainage density) and geoelectrical resistivity survey derived parameters (aquifer resistivity, aquifer thickness, overburden thickness and coefficient of anisotropy). The generated groundwater potential map validated with 74% reliability using groundwater yield of eleven boreholes and eight hand-dug wells was used to microzonate the study area into very low, low, medium and very high groundwater potential zones. The generated groundwater potential distribution information constitutes an asset essential for future development, especially in planning and site selection for heavy or light water demanding establishments within the studied part of the Ibadan metropolis. It also offers very useful information on the regions to focus on for groundwater development to support the inadequate public water supply where applicable.

Fig. 15 Groundwater potential map and BH/HW locations in the area
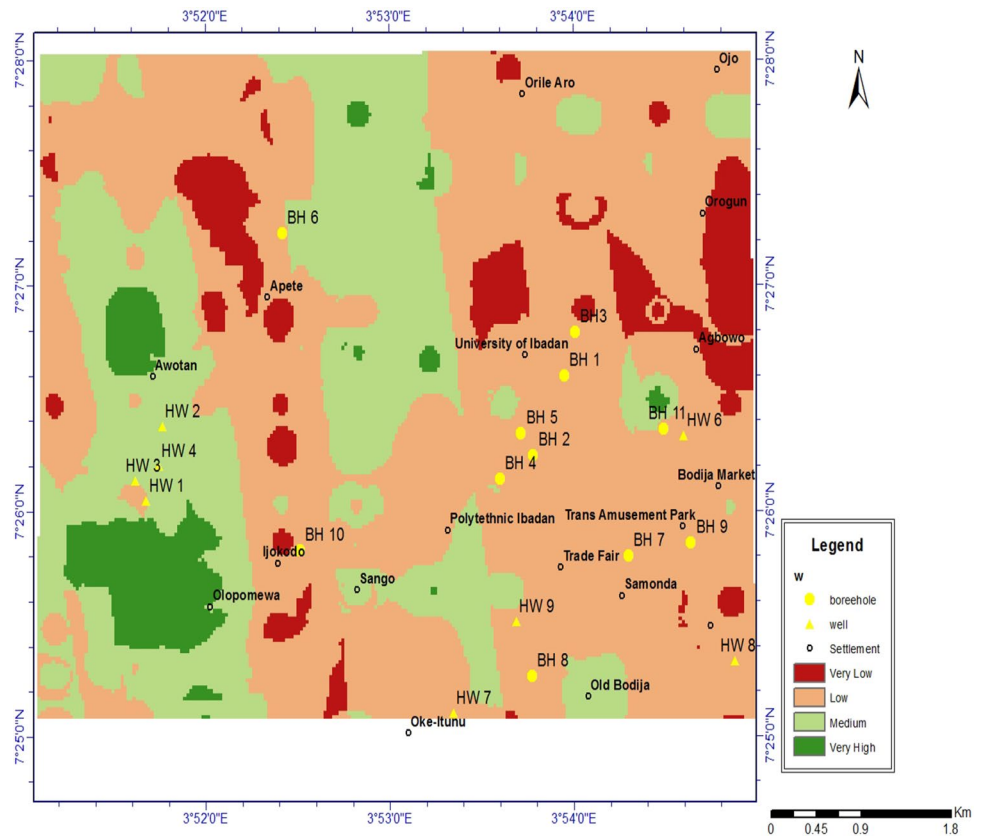
Table 5 Validation of groundwater potential map with borehole yield/hand-dug well data

Borehole/hand-dug well number	Description of yield from groundwater potential map	Yield from pumping test (m³/d)	Yield description from pumping test (m³/d)	Remarks
BH 1	Low	81.6	Medium	Disagree
BH2	Low	86.4	Medium	Disagree
BH3	Low	57.6	Low	Agree
BH 4	Medium	80	Medium	Agree
BH 5	Low	69.1	Low	Agree
BH 6	Low	70	Low	Agree
BH 7	Low	67	Low	Agree
BH 8	Low	72	Low	Agree
BH 9	Low	120	Medium	Disagree
BH 10	Low	64	Low	Agree
BH 11	Low	65	Low	Agree
Hand-dug well number	Description of yield from groundwater potential map	Groundwater yield thickness (m)	Description of yield from hand-dug well	Remarks
HW 1	Low	1.14	Low	Agree
HW 2	Medium	2.73	High	Disagree
HW 3	Medium	2.3	Medium	Agree
HW 4	Medium	1.67	Medium	Agree
HW 5	Low	1.4	Low	Agree
HW 6	Low	1.3	Low	Agree
HW 7	Low	Dry well	Low	Agree
HW 8	Low	2.5	High	Disagree

Compliance with ethical standards

References

Abdullahi M, Yelwa N, Abdulmumin A, Nabage NA (2016) Groundwater exploration in the Basement Complex around Chibok area in Northeastern Nigeria using vertical electrical sounding method. Nigerian J Basic Appl Sci 24(2):37–44

Adiat KAN (2013) Development of models for predicting groundwater resources potential of alluvial aquifer using artificial intelligence techniques. An unpublished Ph.D Thesis. University Sains Malaysia, p 4

Adiat KAN, Osifila AJ, Akinlalu AA, Alagbe O (2018) Mining of geophysical data to predict groundwater prospect in a basement complex terrain of southwestern, Nigeria. Int J Sci Technol Res 7(5):1

Ajibade AC (1980) Geotectonic evolution of the Zungeru Region, Nigeria. Unpubl. PhD thesis, Univ. Wales, Aberystwyth

Akinlalu AA, Adegbuyiro A, Adiat KAN, Akeredolu BE, Lateef WY (2017) Application of multi-criteria decision analysis in prediction of groundwater resources potential: a case of Oke-Ana, Ilesa Area Southwestern, Nigeria. NRIAG J Astron Geophys 6(1):184–200

Burke K, Freeth SJ, Grant NK (1976) The structure and sequence of geological events in the Basement Complex of the Ibadan area, Western Nigeria. Precambrian Res 3:537–545

Chowdhury VM, Rao NH, Sarma PBS (2003) GIS-based decisions support system for groundwater assessment in large irrigation project areas. Agric Water Manag 62:229–252

Fashae OA, Tijani MN, Talabi AO (2014) Delineation of groundwater potential zones in the crystalline basement terrain of SW-Nigeria: an integrated GIS and remote sensing approach. Appl Water Sci 4:19–38. https://doi.org/10.1007/s13201-013-0127-9

Forson AY, Whiteman D (2014) Electrical resistivity characterization of anisotropy in the Biscayne aquifer. Groundwater 52(5):728–736

Grant NK (1969) The late precambrian to early palaeozoic Pan-African orogeny in Ghana, Togo, Dahomey and Nigeria. Geol Soc Am Bull 80:45–56

Grant NK (1970) Geochronology of Precambrian basement rocks from Ibadan, southwestern Nigeria. Earth Planet Sci Lett 10:29–38

Jones HA, Hockey RD (1964) The geology of part of South-Western Nigeria. Bull Geol Surv Nigeria 31:101

Knochenmus LA, Robinson JL (1996) Descriptions of anisotropy and heterogeneity and their effect on groundwater flow and areas of contribution to public supply wells in a karst carbonate aquifer system. USGS Water-Supply Report 47. Reston, Virginia: USGS

Loke MH (2000) Electrical imaging surveys for environmental and engineering studies, a practical guide to 2D and 3D surveys

Malczewski J (1999) GIS and multi criteria decision analysis. John Wiley and Sons, New York

McMurry P (1976) The geology of the Precambrian to Lower Palaeozoic rocks of northern Nigeria-a review. In: Kogbe CA (ed) Geology of Nigeria. Elizabethan Pub Co., Lagos, pp 15–39

Mogaji KA, Lim HS, Abdullah K (2014) Modeling groundwater vulnerability prediction using geographic information system (GIS)-based ordered weighted average (OWA) method and DRASTIC model theory hybrid approach. Arab J Geosci 7:5409–5429. https://doi.org/10.1007/s12517-013-1163-3

U.N SDG 6 (2018) United Nation water's sustainable development goal 6 synthesis report on water and sanitation

Odeyemi IB (1981) A review of orogenic events in the Precambrian Basement of Nigeria, West Africa. Geologische Rundschau 70(3):897–909

Olorunfemi MO (1990) The hydrogeological implication of topographic variation with overburden thickness in Basement Complex Area of Southwestern Nigeria. J Min Geol 26(1):1

Olorunfemi MO, Olarewaju VO, Alade O (1991) On the electrical anisotropy and groundwater yield in a Basement Complex area of Southwestern Nigeria. J Afr Earth Sc 28(2):221–229

Omosuyi GO, Ojo JS, Enikanselu PA (2003) Geophysical investigation for groundwater around Obanla—Obakekere in Akure area within the Basement Complex of South-Western Nigeria. J Min Geol 39(2):109–116

Oyawoye MO (1972) The basement complex of Nigeria. In: Dessauvagie TFJ, Whiteman AJ (eds) African geology. Ibadan Univ. Press, Nigeria, pp 67–99

Oyedele EA, Oyedele TA, Oyedele K (2013) Geo-electrical data analysis to demarcate groundwater pockets in Ado-Ekiti, Southwestern Nigeria. Int J Water Resour Environ Eng 5(11):609–615

Rahaman MA (1976) Review of the basement geology of Southwestern Nigeria. In: Kogbe CA (ed) Geology of Nigeria. Elizabethan Publ Co, Lagos, pp 41–58

Ritzi RW, Andolsek RH (1992) Relation between anisotropic transmissivity and azimuthal resistivity surveys in shallow, fractured, carbonate flow systems. Groundwater 30(5):774–780

Russ W (1957) The geology of parts of Niger, Zaria and Sokoto Provinces, with special reference to the occurrence of gold. Bull Geol Surv Nigeria 27:1

Saaty TL (1977) A scaling method for priorities in hierarchical structures. J Math Psychol 15(3):234–281

Saaty TL (1980) The analytic hierarchy process: planning, priority setting and resources allocation. Mcgraw-Hill, New York

Saaty TL (1990) How to make a decision: the analytic hierarchy process. Eur J Oper Res 48(1):9–26

Tecle A, Duckstein L (1994) Concepts of multicriteria decision making. In: Bogardi JJ, Nachtnebel HP (eds) Multicriteria analysis in water resources management. UNESCO, Paris, pp 33–62

Toteu SF, Bertrand JM, Penaye J, Macaudiere J, Angoua S, Barbey P (1991) Cameroon: a tectonic keystone in the Pan-African network. In: Lewry JF, Stauffer MR (eds) The early Proterozoic Trans-Hudson Orogeny of north America: Special paper 37. Geological Association of Canada, Canada, pp 483–496

United Nations world water assessment Programme (2015) The United Nations world water development report 2015: water for a sustainable world. UNESCO, Paris